ELSEVIER

Biophysical Chemistry 70 (1998) 247–257

Biophysical Chemistry

Irreversible thermal denaturation of uridine phosphorylase from *Escherichia coli* K-12

A.E. Lyubarev [a,*], B.I. Kurganov [a], A.A. Burlakova [b], V.N. Orlov [c]

[a] *Bach Institute of Biochemistry, Russian Academy of Sciences, Leninsky prospekt, 33, Moscow 117071, Russian Federation*
[b] *State Research Institute of Genetics and Selection of Industrial Microorganisms, 1 Dorozhny proezd, 1, Moscow 113545, Russian Federation*
[c] *Belozersky Institute of Physico–Chemical Biology, Lomonosov Moscow State University, Moscow 119899, Russian Federation*

Received 20 June 1997; revised 13 November 1997; accepted 17 November 1997

Abstract

Thermal denaturation of uridine phosphorylase from *Escherichia coli* K-12 has been studied by differential scanning calorimetry. The excess heat capacity vs. temperature profiles were obtained at temperature scanning rates of 0.25, 0.5, and 1 K/min. These profiles were analysed using three models of irreversible denaturation which are approximations to the whole Lumry–Eyring model, namely, the one-step model of irreversible denaturation, the Lumry–Eyring model with the fast equilibrating first step, and the model involving two consecutive irreversible steps. In terms of statistics the latter model describes the kinetics of thermal denaturation of uridine phosphorylase more satisfactorily than the two other models. The values of energy activation for the first and second steps calculated for the model involving two consecutive irreversible steps are the following: $E_{a,1} = 609.3 \pm 1.8$ kJ/mol and $E_{a,2} = 446.8 \pm 3.2$ kJ/mol. © 1998 Elsevier Science B.V.

Keywords: Protein denaturation; Differential scanning calorimetry; Uridine phosphorylase

1. Introduction

Thermal denaturation of proteins is being studied intensively today. Investigation of denaturation may help to elucidate the mechanisms of the reverse process, i.e., protein folding.

Differential scanning calorimetry (DSC) is a powerful technique to study thermal denaturation. It allows investigators to get valuable information on thermodynamic and kinetic features of the process [1–7]. Therefore, elaboration of mathematical methods for analysis of DSC curves is of great importance.

The Lumry–Eyring model [8] is the most attractive model for protein thermal denaturation. It involves a reversible unfolding step followed by an irreversible denaturation step:

$$\mathrm{N} \underset{k_{-1}}{\overset{k_1}{\rightleftarrows}} \mathrm{U} \overset{k_2}{\rightarrow} \mathrm{D} \qquad (1)$$

where N, U, and D are the native, conformationally changes (possibly partially unfolded), and denatured forms of the protein, respectively. At the same time, it is known that DSC data for denaturation of some proteins are satisfactorily described by the model

* Corresponding author. Fax: +7-095-954-2732; e-mail: inbio@glas.apc.org.

PII S0301-4622(97)00133-6

involving the reversible step only [1]. Such a model may be considered as a special case of the Lumry–Eyring model if the irreversible step does not occur within the temperature range under investigation.

Nevertheless, thermal denaturation of a great many proteins is irreversible [6,7,9]. In this case it is necessary to use the models of irreversible denaturation for analysis of DSC curves. However, there are some problems with the use of the whole Lumry–Eyring model, as the system of differential equations describing it cannot be solved at varying temperature.

The present paper deals with thermal denaturation of uridine phosphorylase (EC 2.4.2.3) from *Escherichia coli* K-12. The enzyme catalyses phosphorolysis of uridine with formation of ribose-1-phosphate and uracil [10,11]. The molecule of uridine phosphorylase is a hexamer composed of six identical subunits with a molecular mass of 27.5 kDa [12–14]. According to the X-ray data [15,16], the hexamer consists of three structurally formed dimers whose monomers are connected by the symmetry axis of the second order, and three dimers link by the symmetry axis of the third order.

The aim of the present paper is to investigate the thermal denaturation of uridine phosphorylase by the DSC method and to use the models, which are approximations to the whole Lumry–Eyring model, for analysis of thermal denaturation of the enzyme.

2. Models

2.1. The one-step model of irreversible denaturation

The simplest model of irreversible protein denaturation is a monomolecular transformation of native protein to the denatured state with the rate constant of the first order k:

$$\mathrm{N} \xrightarrow{k} \mathrm{D} \qquad (2)$$

In application to DSC data this model was investigated by Sanchez-Ruiz and Mateo [5], Freire et al. [6], Sanchez-Ruiz et al. [17], Conejero-Lara et al. [18], Sanchez-Ruiz [19], and Kurganov et al. [20]. The excess heat capacity (C_p^{ex}) can be expressed as a function of absolute temperature (T) at the constant scanning rate $\upsilon = \mathrm{d}T/\mathrm{d}t$ (t is time) [5,6,20]:

$$C_p^{ex} = \frac{1}{\nu}\Delta H \exp\left\{\frac{E_a}{R}\left(\frac{1}{T^*} - \frac{1}{T}\right)\right\} \times \exp\left\{-\frac{1}{\nu}\int_{T_0}^{T}\exp\left[\frac{E_a}{R}\left(\frac{1}{T^*} - \frac{1}{T}\right)\right]\mathrm{d}T\right\} \qquad (3)$$

where ΔH is the enthalpy of denaturation, E_a is the energy of activation for the denaturation process, T^* is the temperature at which $k = 1\ \mathrm{min}^{-1}$.

Model (2) was used for the quantitative description of thermal denaturation of some proteins [17,18,21–27]. Kurganov et al. [20] discussed the criteria of validity of the model and showed that the thermal denaturation of several proteins, described earlier in the context of the one-step irreversible model, does not strictly follow it.

2.2. The Lumry–Eyring model with the fast equilibrating first step

The model, in which the rate of equilibrium establishing for the first step is high in comparison with that of the second step, may be considered as an approximation to the whole Lumry–Eyring model [19,28–30]:

$$\mathrm{N} \overset{K}{\rightleftarrows} \mathrm{U} \xrightarrow{k_2} \mathrm{D} \qquad (4)$$

Milardi et al. [29] have obtained the expression for C_p^{ex} for this model:

$$C_p^{ex} = \left[\frac{K\Delta H_u}{(K+1)^2}\left(\frac{k}{\nu} + \frac{\Delta H_u}{RT^2}\right) + \Delta H_i \frac{1}{\nu}\frac{kK}{K+1}\right] \times \exp\left(-\frac{1}{\nu}\int_{T_0}^{T}\frac{kK}{K+1}\mathrm{d}T\right) \qquad (5)$$

where ΔH_u is the change of enthalpy associated with the first step, ΔH_i is the change of enthalpy associated with the second step, K is the equilibrium constant for the first step ($K = \exp[-\Delta H_u/R\ (1/T - 1/T_{1/2})]$), k is the rate constant for the second step ($k = \exp[-E_a/R\ (1/T - 1/T^*)]$); $T_{1/2}$ is the temperature at which $K = 1$, T^* is the temperature at which $k = 1\ \mathrm{min}^{-1}$.

The model was used for the quantitative description of thermal denaturation of azurin [29,31,32]. However, the results of fitting of Eq. (5) to the DSC curves testify to only rough description of the experimental data.

2.3. The model involving two consecutive irreversible steps

The model involving two consecutive irreversible steps can be considered as another approximation to the whole Lumry–Eyring model (in this case we suppose that $k_{-1} \ll k_2$, see model (1)):

$$\mathrm{N} \xrightarrow{k_1} \mathrm{U} \xrightarrow{k_2} \mathrm{D} \qquad (6)$$

We have obtained the following expression for C_p^{ex} for this model (see Appendix A):

$$C_p^{ex} = \frac{\Delta H_1 k_1}{\nu} \exp\left(-\frac{1}{\nu}\int_{T_0}^{T} k_1 \mathrm{d}T \right) + \frac{\Delta H_2 k_2}{\nu^2} \exp\left(-\frac{1}{\nu}\int_{T_0}^{T} k_2 \mathrm{d}T \right) \times \int_{T_0}^{T} \left[k_1 \exp\left(\frac{1}{\nu}\int_{T_0}^{T} (k_2 - k_1)\mathrm{d}T \right) \right] \mathrm{d}T \qquad (7)$$

where ΔH_1 and ΔH_2 are changes of enthalpy for the first and second steps, k_1 and k_2 are the rate constants for the first and second steps: $k_1 = \exp[-E_{a,1}/R \ (1/T - 1/T_1^*)]$, $k_2 = \exp[-E_{a,2}/R \ (1/T - 1/T_2^*)]$; T_1^* and T_2^* are the temperatures at which the rate constants k_1 and k_2 are equal to 1 min^{-1}.

3. Methods

Uridine phosphorylase was prepared from *E. coli* K-12 (the superproducer of the enzyme) by the method described in [33] using 1 mM 2-mercaptoethanol to protect the sulphydryl groups of the enzyme from oxidation. The enzyme preparation was homogeneous according to the results of electrophoresis in polyacrylamide gel [34]. The protein concentration was determined spectrophotometrically using the absorbance index 0.67 cm^{-1} for 0.1%-solution at 280 nm [35] or by the Bradford assay [36].

Calorimetric study was carried out by means of a DASM-4 microdifferential scanning calorimeter (Scientific and Industrial Association 'Biopribor', Russian Academy of Sciences) equipped with 0.47-ml capillary platinum cells. To obtain DSC curves, the solution of uridine phosphorylase 0.95 mg/ml in 50 mM Hepes–NaOH, pH 7.55, was scanned from 20 to 80°C with scanning rates of 0.25, 0.5 and 1 K/min.

All the experimental points were used for quantitative analysis of the DSC curves. To fit the theoretical curves to the experimental data we used an original program for IBM-compatible computer based on the minimization algorithm by Nelder and Meed [37]. In the cases when the chemical baseline was preliminarily subtracted, the procedure proposed by Takahashi and Sturtevant [38] was used. The standard error of parameter estimation was calculated as described in Ref. [39]. The correlation coefficient r used as a criterion for the accuracy of fitting was calculated by the equation:

$$r = \sqrt{1 - \sum_{i=1}^{n} \left(y_i - y_i^{calc} \right)^2 / \sum_{i=1}^{n} \left(y_i - y_i^{m} \right)^2} \qquad (8)$$

where y_i and y_i^{calc} are the experimental and calculated values of C_p^{ex}, respectively, y_i^{m} is the mean experimental value of C_p^{ex}, n is the number of points.

4. Results

4.1. DSC profiles of uridine phosphorylase

Heat capacity vs. temperature profiles were obtained for scanning rates of 0.25, 0.5 and 1 K/min. The position of a maximum on the profiles is shifted to higher temperatures with the scanning rate. Such an effect testifies to the irreversible character of thermal denaturation of the protein [5,6]. Therefore, to analyse the profiles obtained we used the models of irreversible denaturation of protein.

4.2. The one-step model of irreversible denaturation

To obtain the excess heat capacity (C_p^{ex}) vs. temperature profile, it is necessary to subtract the chemi-

Table 1
Arrhenius equation parameter estimates for one-step model (2) of thermal denaturation of uridine phosphorylase

Parameter[a]	Version[b]	Temperature scanning rate, K/min			Fitting to all curves
		0.25	0.5	1	
E_a, kJ/mol	−BL	650.7 ± 2.1	628.5 ± 1.7	560.4 ± 1.1	577.8 ± 1.2
	+BL	642.5 ± 2.1	617.8 ± 1.4	562.1 ± 1.0	573.9 ± 1.2
T^*, K	−BL	334.7 ± 0.01	335.0 ± 0.01	335.5 ± 0.01	335.3 ± 0.01
	+BL	334.7 ± 0.01	335.0 ± 0.01	335.5 ± 0.00	335.3 ± 0.01
ΔH, kJ/mol	−BL	1983 ± 5	2226 ± 5	2641 ± 4	
	+BL	2026 ± 5	2275 ± 4	2642 ± 4	
r[c]	−BL	0.9970	0.9977	0.9988	0.9944
	+BL	0.9971	0.9983	0.9989	0.9947

[a] The estimates ± standard errors are given.
[b] −BL: chemical baseline was preliminarily subtracted; +BL: chemical baseline was inserted in the expression for C_p.
[c] Correlation coefficient (r) is calculated by Eq. (8).

cal baseline which takes into consideration the difference between heat capacities of the initial and final protein states [7,38]. At the same time, the primary C_p vs. temperature profile could be analysed without preliminary subtraction of the chemical baseline. The expression for C_p may be obtained by insertion of the corresponding terms describing the chemical baseline in Eq. (3) for C_p^{ex}:

$$C_p = C_p^{ex} + C_p^N\gamma_N + C_p^D(1-\gamma_N) \quad (9)$$

where C_p^N and C_p^D are heat capacities of the native and denatured protein, γ_N is the mole fraction of the native state: $\gamma_N = \exp(-1/v\int_{T_0}^{T} k\mathrm{d}T)$. It is assumed that C_p^N and C_p^D are linear functions of temperature and described by the equation $C_p^x = \alpha_\times + \beta_x T$ (x is N or D), where α_x and β_x are parameters which can be obtained by the linear approximation of the initial (for C_p^N) and final (for C_p^D) parts of the DSC profile.

The results of fitting of Eqs. (3) and (9) to the experimental data are shown in Table 1 (lines −BL and +BL, respectively). As can be seen from the table, the results of both versions of fitting do not

Table 2
Arrhenius equation parameter estimates for Lumry–Eyring model with fast equilibrating first step (4) of thermal denaturation of uridine phosphorylase

Parameter[a]	Version[b]	Temperature scanning rate, K/min			Fitting to all curves
		0.25	0.5	1	
ΔH_i, kJ/mol	−BL	1408 ± 9	1587 ± 12	2470 ± 10	1742 ± 979
	+BL	4426 ± 172	3994 ± 976	2929 ± 29	4155 ± 36
ΔH_u, kJ/mol	−BL	555.4 ± 7.1	628.8 ± 12.8	265.2 ± 8.0	184.0 ± 44.3
	+BL	674.1 ± 26.1	517.1 ± 10.8	420.0 ± 9.4	751.7 ± 4.4
E_a, kJ/mol	−BL	293.7 ± 65.0	157.2 ± 26.7	517.2 ± 2.5	426.7 ± 57.9
	+BL	321.3 ± 23.5	218.5 ± 43.4	414.0 ± 12.6	389.8 ± 1.7
$T_{1/2}$	−BL	332.8 ± 0.7	334.3 ± 0.2	329.5 ± 0.2	340.6 ± 3.0
	+BL	330.6 ± 0.4	334.0 ± 0.5	332.3 ± 0.4	329.7 ± 0.03
T^*	−BL	335.1 ± 0.1	334.1 ± 0.3	335.2 ± 0.01	332.4 ± 1.6
	+BL	336.2 ± 0.1	334.2 ± 0.6	335.1 ± 0.1	335.7 ± 0.01
r[c]	−BL	0.9990	0.9994	0.9994	0.9945
	+BL	0.9995	0.9998	0.9998	0.9997

[a] The estimates ± standard errors are given.
[b] −BL: chemical baseline was preliminarily subtracted; +BL: chemical baseline was inserted in the expression for C_p.
[c] Correlation coefficient (r) is calculated by Eq. (8).

significantly diverge for this model. At the same time, the estimates of the parameters vary significantly with the varying scanning rate. This means that the model cannot be used for the description of thermal denaturation of uridine phosphorylase [20].

4.3. Two-step models of irreversible denaturation

Since the one-step model is not applicable to thermal denaturation of uridine phosphorylase, we have used two two-step models, namely, the Lumry–Eyring model with the fast equilibrating first step (4) described by Eq. (5) and the model involving two consecutive irreversible steps (6) described by Eq. (7).

The results of fitting of Eqs. (5) and (7) to the experimental data are shown in Tables 2 and 3 (lines −BL), respectively. One can see that the accuracy of fitting (as indicated by the values of r) is significantly higher than in case of the one-step model (2). This seems to be due to the increase in the number of parameters, namely, from three in Eq. (3) to five in Eq. (5) and six in Eq. (7). The standard errors of parameter estimation rise simultaneously; this effect is also due to the increase in the number of parameters.

The most important result of fitting is that the estimates of the parameters vary significantly with the scanning rate. The divergence is much higher than in the case of model (2).

4.4. Effect of heat capacity of the intermediate state

As we have stated in Section 4.2, the direct insertion of the chemical baseline in the expression for C_p, instead of its preliminary subtraction, has no significant effect on the results of fitting for one-step model (2). However, this is not true for the models taking into consideration an intermediate state. The character of the chemical baseline depends on unknown heat capacity of the intermediate state, therefore the shape of the line can significantly differ from the sigmoidal curve of Takahashi–Sturtevant [38].

To directly analyse the C_p vs. T profile for models (4) and (6), we should modify Eqs. (5) and

Table 3
Arrhenius equation parameter estimates for model including two consecutive irreversible steps (6) of thermal denaturation of uridine phosphorylase

Parameter[a]	Version[b]	Temperature scanning rate, K/min			Fitting to all curves[c]	
		0.25	0.5	1	Variant 1	Variant 2
$E_{a,1}$, kJ/mol	−BL	735.3 ± 7.1	661.2 ± 9.1	440.4 ± 10.6	609.3 ± 1.8	636.8 ± 2.0
	+BL	649.7 ± 36.1	616.3 ± 20.3	292.2 ± 8.3	494.2 ± 2.0	
$E_{a,2}$, kJ/mol	−BL	555.5 ± 34.9	374.0 ± 34.6	555.7 ± 16.3	446.8 ± 3.2	452.6 ± 3.1
	+BL	431.4 ± 31.5	237.5 ± 86.0	508.0 ± 4.2	457.4 ± 0.7	
ΔH_1, kJ/mol	−BL	1037 ± 111	1092 ± 140	1317 ± 120		636 ± 27
	+BL	843 ± 1988	1083 ± 1147	1098 ± 464	417 ± 6	
ΔH_2, kJ/mol	−BL	935 ± 112	1138 ± 139	1374 ± 122		
	+BL	1694 ± 552	1492 ± 801	2391 ± 22	2781 ± 8	
$\Delta H_2/\Delta H_1$	−BL	0.90 ± 0.20	1.04 ± 0.26	1.04 ± 0.19	3.82 ± 0.16	
	+BL	2.01 ± 5.39	1.38 ± 2.20	2.18 ± 0.94	6.68 ± 0.11	
T_1^*	−BL	333.4 ± 0.07	334.1 ± 0.04	335.7 ± 0.01	333.4 ± 0.04	333.5 ± 0.04
	+BL	333.4 ± 0.80	334.4 ± 0.25	335.9 ± 0.07	333.2 ± 0.02	
T_2^*	−BL	335.3 ± 0.10	335.9 ± 0.07	334.0 ± 0.08	335.6 ± 0.01	335.6 ± 0.01
	+BL	335.8 ± 0.13	336.2 ± 0.20	334.9 ± 0.04	335.5 ± 0.00	
r[d]	−BL	0.9992	0.9993	0.9994	0.9986	0.9984
	+BL	0.9995	0.9997	0.9998	0.9996	

[a] The estimates ± standard errors are given.
[b] −BL: chemical baseline was preliminarily subtracted; +BL: chemical baseline was inserted in the expression for C_p.
[c] Variant 1: $\Delta H_2/\Delta H_1$ is global parameter; variant 2: ΔH_1 is global parameter.
[d] Correlation coefficient (r) is calculated by Eq. (8).

(7) by analogy with Eq. (9) in Section 4.2:

$$C_p = C_p^{ex} + C_p^N\gamma_N + C_p^U\gamma_U + C_p^D(1 - \gamma_N - \gamma_U), \quad (10)$$

where γ_N and γ_U are the mole fraction of the native and intermediate states, C_p^{ex} is excess heat capacity calculated by Eq. (5) or Eq. (7), C_p^N, C_p^D, and C_p^U are heat capacities of the native, denatured, and intermediate states, respectively. (We suppose that C_p^U, as well as C_p^N and C_p^D, can be described by the linear expression $C_p^U = \alpha_U + \beta_U T$.) For model (4) the fraction of the native state is expressed as follows:

$$\gamma_N = \frac{1}{K+1}\exp\left(-\frac{1}{\nu}\int_{T_0}^{T}\frac{kK}{K+1}dT\right), \quad (11)$$

and the fraction of the intermediate state is defined by the formula:

$$\gamma_U = \frac{K}{K+1}\exp\left(-\frac{1}{\nu}\int_{T_0}^{T}\frac{kK}{K+1}dT\right). \quad (12)$$

For model (6) we get the following expressions for the fractions of the native and intermediate states:

$$\gamma_N = \exp\left(-\frac{1}{\nu}\int_{T_0}^{T}k_1dT\right), \quad (13)$$

$$\gamma_U = \frac{1}{\nu}\exp\left(-\frac{1}{\nu}\int_{T_0}^{T}k_2dT\right) \times\int_{T_0}^{T}\left[k_1\exp\left(\frac{1}{\nu}\int_{T_0}^{T}(k_2-k_1)dT\right)\right]dT \quad (14)$$

(see Appendix A).

The results of fitting of Eq. (10) to the experimental data are also shown in Tables 2 and 3 (lines +BL). One can see that in all the cases the accuracy of fitting rises as compared to the analogous cases with the preliminary subtracted baseline. However, the standard errors of parameter estimation increase too. At the same time, the marked divergence of parameter estimates for different scanning rates is retained.

It should be noted that there is a sharp increase in the values of the total change of enthalpy, which is due to the fact that the calculated values of C_p^U have proved to be much lower than the corresponding values of C_p^N and C_p^D for all the scanning rates and for both models. Our calculations show that, as a result, the baseline takes the shape of an inverted bell.

4.5. Simultaneous fitting to all the curves

Since fitting of the theoretical expressions to the experimental DSC curves corresponding to the different scanning rates results in different parameter estimates, it is necessary to fit the theoretical expressions to all the experimental curves simultaneously. However, there is a problem connected with the difference in the values of denaturation enthalpy.

As can be seen from Tables 1–3, the total denaturation enthalpy (ΔH in Table 1, $\Delta H_u + \Delta H_i$ in Table 2, $\Delta H_1 + \Delta H_2$ in Table 3) has significantly different values for the different scanning rates. In the case of fitting to experimental curves after the preliminary subtraction of baseline, these values are virtually identical for all the models and determined by the area under the C_p^{ex} vs. T profile.

Some differences in the values of denaturation enthalpy measured at varying scanning rates were observed in a number of works [17,18,25–27,31,40,41]. The reason for the differences remains unclear. Denaturation enthalpy is not to depend on the scanning rate if protein concentration, as well as the initial and final states are identical in the experiments with varying scanning rates. One of the possible reason is the difference in protein concentration due to inaccuracy in solution preparation. The fact that there is no common tendency in the character of dependence of the denaturation enthalpy value on the scanning rate testifies in favour of this assumption. Thus, for lentil lectin [27], azurin from *Pseudomonas aeruginosa* [31], and bovine superoxide dismutase [40] as well as for uridine phosphorylase the values of ΔH increased with the scanning rate. The reverse tendency was observed for cellulase from *Streptomyces halstedii* JM8 [26]. In the case of acetylcholinesterase from *Torpedo californica* [25], thermolysin from *Bacillus thermoproteolyticus rokko* [17] and glucosamine-6-phosphate deaminase from *E. coli* [41], the maximum values of ΔH were noted for intermediate rates. In the case of porcine pancreatic procarboxypeptidase B and carboxypeptidase B [18] the ΔH vs. ν dependence varied with pH.

Another possible reason is the difference between

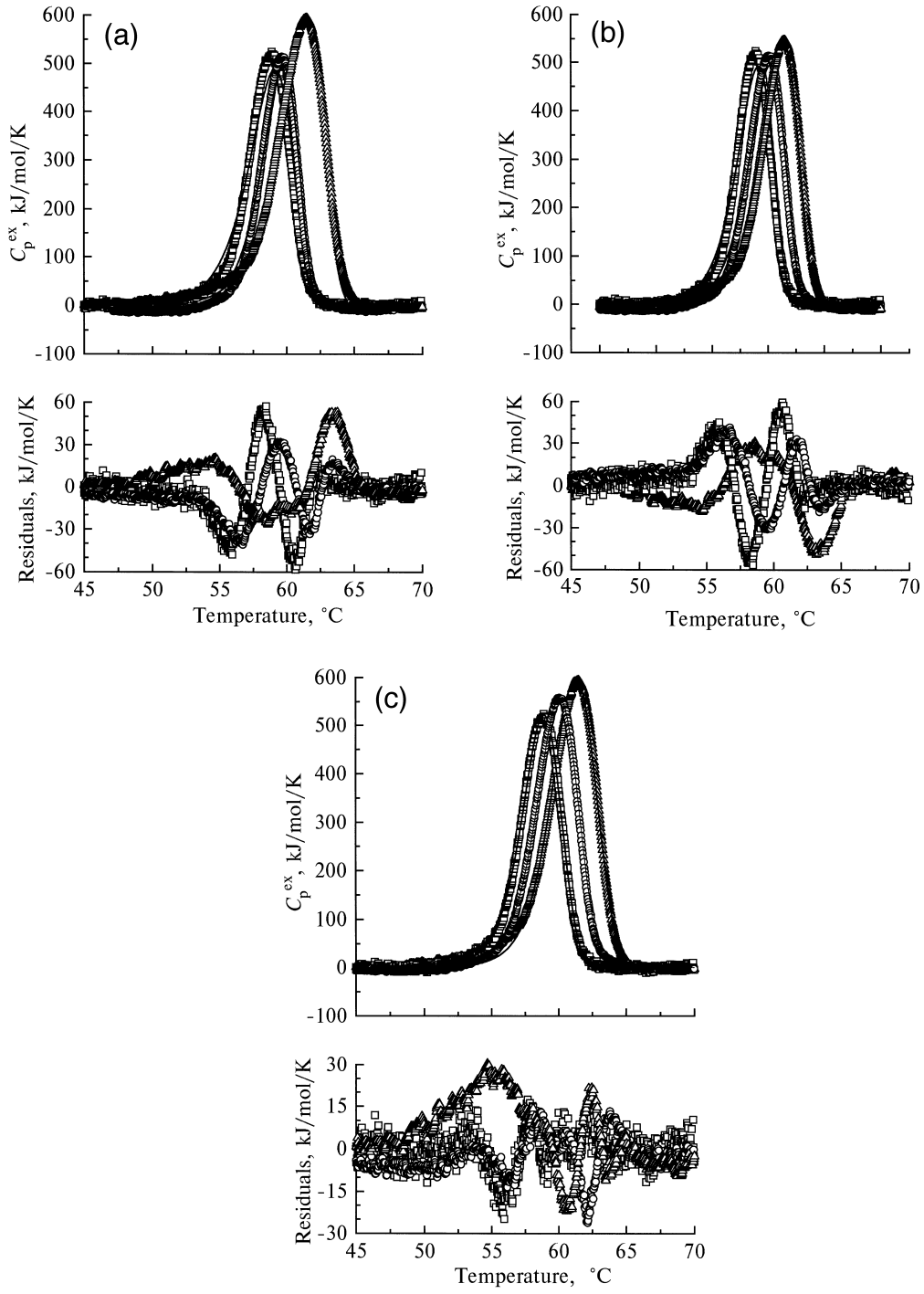

Fig. 1. Results of fitting of the theoretical equations to the experimental C_p^{ex} vs. temperature profiles obtained for uridine phosphorylase from *E. coli* at scanning rates 0.25 (squares), 0.5 (circles) and 1 (triangles) K/min: (a) the one-step model (Eq. (3)), (b) the Lumry–Eyring model with the fast equilibrating first step (Eq. (5)), and (c) the model involving two consecutive irreversible steps (Eq. (7)). Solid lines in the upper plots are the best fits. Curves at the lower plots are residuals.

the final states of protein reached at different scanning rates. Such a situation is realized, for example, when denaturation is accompanied by the formation of aggregates whose form depends on the rate of denaturation, i.e., on the scanning rate. Theoretical description of this phenomenon is very difficult.

The third possible reason is incorrect tracing of the chemical baseline.

Taking all the above facts into consideration we have carried out fitting of the theoretical formulas corresponding to each model simultaneously to all the experimental curves in two versions. In the first version we preliminary subtracted chemical baseline, while in the second one we included the baseline in the equation for C_p. For model (2), E_a and T^* were estimated as global parameters, whereas the optimal values of ΔH were calculated for each curve individually. For model (4) the five parameters used for fitting to individual curves were estimated as global ones; while in the case of the version with preliminary subtraction of the baseline, an additional multiplier individual for each curve was introduced.

For model (6) in the version with preliminary subtraction of the baseline, the fitting was carried out in two ways. In the first case, $\Delta H_2/\Delta H_1$ was a global parameter, whereas ΔH_1 and ΔH_2 retained individual values. In the second case, ΔH_1 was a global parameter, whereas ΔH_2 had individual values. In the version with insertion of the baseline in the expression for C_p, all six parameters were estimated as global ones.

The results of fitting of the theoretical expressions to all the experimental curves are shown in the right-hand columns of Tables 1–3. For models (2) and (4) in the version with preliminary subtraction of the baseline, the accuracy of fitting proved to be low (see also Fig. 1a and b). For model (6) the accuracy of fitting was significantly higher for both cases (Fig. 1c shows the results of fitting with the global value of the ratio $\Delta H_2/\Delta H_1$, for the second case the picture is similar). It should be noted that the parameter estimates proved to be close in both cases (only for $E_{a,1}$ we can note a significant difference).

As was to be expected for model (2), the insertion of the baseline in the expression for C_p did not result in significant alterations. For model (6) and especially for model (4), the accuracy of fitting significantly increased. Simultaneously, the values of the total enthalpy changes rise as in the cases of fitting to individual curves [especially for model (4)].

5. Discussion

In the present work, we have attempted to describe thermal denaturation of uridine phosphorylase from *E. coli* using three kinetic models which can be considered as approximations to the whole Lumry–Eyring model (1). We have found that model (2) including one irreversible step is not applicable to description of C_p^{ex} vs. temperature profiles for this enzyme. Therefore, two or more steps and, hence, one or more intermediate states can be postulated.

The applicability of the two two-step models has been also discussed in the present paper. In the first case [the Lumry–Eyring model with the fast equilibrating first step (4)] it is assumed that the second step is rate limiting. In the second case [the model involving two consecutive irreversible steps (6)] it is assumed that the rate of the reverse reaction for the first step is significantly less than that of the second reaction.

Analysis of the results obtained shows that in terms of statistics model (6) involving two consecutive irreversible steps more satisfactorily describes the kinetics of thermal denaturation of uridine phosphorylase than the Lumry–Eyring model with the fast equilibrating first step (4).

Eq. (7) gives a satisfactory approximation to the experimental data even in the case of simultaneous fitting to all the curves. Nevertheless, the initial parts of the C_p^{ex} vs. temperature profiles of the theoretical curves are slightly lower than those of the experimental curves (see Fig. 1c). It is evident that the approximation is not absolutely precise. Apparently, the use of the whole Lumry–Eyring model would provide a higher accuracy.

The cause of the difference in the values of denaturation enthalpy calculated at different scanning rates remains unclear. In the present work we have used different variants of mathematical treatment taking into consideration some possible causes of this difference. In particular, we assumed that the shape of the chemical baseline could change owing to a contribution of an unknown heat capacity of the intermediate state. However, when heat capacity of

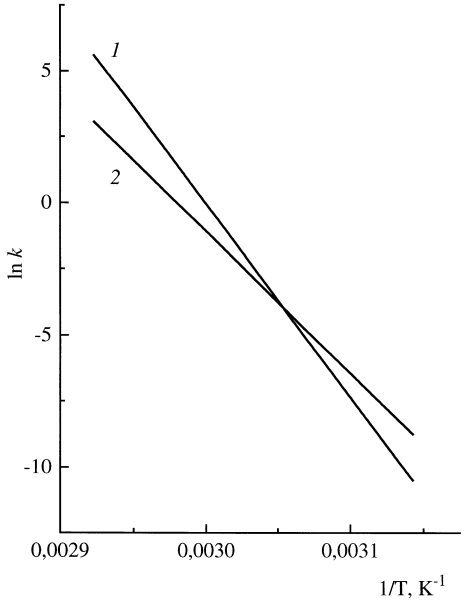

Fig. 2. Dependence of the rate constants for the first and second denaturation steps on the reciprocal temperature in semi-logarithmic coordinates for model (6). The values of Arrhenius equation parameters ($E_{a,1} = 609.3$ kJ/mol, $E_{a,2} = 446.8$ kJ/mol, $T_1^* = 333.4$ K, $T_2^* = 335.6$ K) are taken from the results of simultaneous fitting to all the curves with the preliminary subtracted chemical baseline (see Table 3). The first and second step of the denaturation process are referred to as 1 and 2, respectively.

the intermediate state was taken into account as one of the parameters under estimation, its value found by fitting proved to be significantly lower than heat capacities of the initial and final states. The physical sense of this phenomenon is hard to explain.

For the model involving two consecutive irreversible steps simultaneous fitting to all the curves was carried out using two approaches. In the first case we maintained the ratio of enthalpy absorbed at both the steps as a common parameter for all the scanning rates assuming that the difference in the values of enthalpy for different scanning rates was associated with some scale factor (for example, with the difference in real protein concentrations). In the second case the value of enthalpy of the first step was maintained constant on the assumption that there are side effects at the second step. However, both approaches have resulted in similar values of the parameter estimates and the correlation coefficient.

The analysis of the results shown in Tables 2 and 3 demonstrates that both denaturation steps are accompanied by an appreciable thermal effect, but the thermal effect of the second step is higher. The value of the ratio is different for the two models and for the different modes of analysis, but the general tendency is evident. The results shown in Table 3 also demonstrate that the activation energy for the first step is higher than that for the second one, whereas the value of T^* is higher for the second step as compared to the first one. This means that at relatively low temperatures the rate constant for the first step k_1 is lower than that for the second step k_2 (see Fig. 2), i.e., the first step is rate limiting. When temperature rises (above 54–55°C for the parameters calculated on simultaneous fitting to all the curves with the preliminary subtracted baseline), the value of k_1 becomes higher than the value of k_2, and the second step becomes rate limiting.

It is interesting that on simultaneous fitting to all the curves, the activation energy for the second step for models (4) and (6) has proved to be approximately identical. Its value is about 450 kJ/mol.

Acknowledgements

We are grateful to Dr. D.R. Davydov for the assistance in preparing the computer program. The study was funded by grants 96-04-50819 and 96-04-10016C from the Russian Foundation for Fundamental Research.

Appendix A

The kinetic behaviour of the system described by model (6) is determined by the system of differential equations.

$$\begin{cases} \dfrac{d\gamma_N}{dt} = -k_1\gamma_N \\ \dfrac{d\gamma_U}{dt} = k_1\gamma_N - k_2\gamma_U \end{cases} \quad (A.1)$$

If the scanning rate is constant ($v = dT/dt$), the system (A.1) assumes the form

$$\begin{cases} \dfrac{d\gamma_N}{dT} = -\dfrac{1}{v}k_1\gamma_N \\ \dfrac{d\gamma_U}{dT} = \dfrac{1}{v}(k_1\gamma_N - k_2\gamma_U) \end{cases} \quad (A.2)$$

The first equation of system (A.2) is solved as in the

case of model (2) [20], hence

$$\gamma_N = \exp\left(-\frac{1}{\nu}\int_{T_0}^{T} k_1 dT \right). \quad (A.3)$$

Substituting Eq. (A.3) into the second equation of system (A.2), we obtain

$$\frac{d\gamma_U}{dT} + \frac{k_2}{\nu}\gamma_U = \frac{k_1}{\nu}\exp\left(-\frac{1}{\nu}\int_{T_0}^{T} k_1 dT \right). \quad (A.4)$$

Eq. (A.4) is linear. Solving it and taking into consideration that $\gamma_U = 0$ at $T = T_0$, we obtain

$$\gamma_U = \frac{1}{\nu}\exp\left(-\frac{1}{\nu}\int_{T_0}^{T} k_2 dT \right) \times \int_{T_0}^{T}\left[k_1 \exp\left(\frac{1}{\nu}\int_{T_0}^{T}(k_2 - k_1)dT \right)\right] dT. \quad (A.5)$$

The excess enthalpy change of the reaction $\langle \Delta H \rangle$ is equal to the sum of the excess enthalpy changes of both steps

$$\langle \Delta H \rangle = \Delta H_1(1 - \gamma_N) + \Delta H_2(1 - \gamma_N - \gamma_U). \quad (A.6)$$

Taking into consideration system (A.2), the excess heat capacity is expressed as

$$C_p^{ex} = \frac{d\langle \Delta H \rangle}{dT} = \frac{\Delta H_1 k_1}{\nu}\gamma_N + \frac{\Delta H_2 k_2}{\nu}\gamma_U. \quad (A.7)$$

Substituting Eqs. (A.3) and (A.5) into Eq. (A.7), we obtain the final expression for the C_p^{ex} vs. temperature profile:

$$C_p^{ex} = \frac{\Delta H_1 k_1}{\nu} \times \exp\left(-\frac{1}{\nu}\int_{T_0}^{T} k_1 dT \right) + \frac{\Delta H_2 k_2}{\nu^2}\exp\left(-\frac{1}{\nu}\int_{T_0}^{T} k_2 dT \right) \times \int_{T_0}^{T}\left[k_1 \exp\left(\frac{1}{\nu}\int_{T_0}^{T}(k_2 - k_1)dT \right)\right] dT. \quad (A.8)$$

References

[1] P.L. Privalov, Adv. Protein Chem. 33 (1979) 167.
[2] P.L. Mateo, in: R. da Silva (Ed.), Thermochemistry and Its Applications to Chemical and Biochemical Systems, Reidel, Dordrecht, 1984, p. 541.
[3] P.L. Privalov, S.A. Potekhin, Methods in Enzymology, Vol. 131, Academic Press, New York, 1986, p. 4.
[4] J.M. Sturtevant, Annu. Rev. Phys. Chem. 38 (1987) 463.
[5] J.M. Sanchez-Ruiz, P.L. Mateo, Cell Biol. Rev. 11 (1987) 15.
[6] E. Freire, W.W. van Osdol, O.L. Mayorga, J.M. Sanchez-Ruiz, Annu. Rev. Biophys. Biophys. Chem. 19 (1990) 159.
[7] J.M. Sanchez-Ruiz, in: B.B. Biswas, S. Roy (Eds.), Proteins: Structure, Function, and Engineering (Subcellular Biochemistry, Vol. 24), Plenum, New York, 1995, p. 133.
[8] R. Lumry, H. Eyring, J. Phys. Chem. 58 (1954) 110.
[9] A.M. Klibanov, T.J. Ahern, in: D.L. Oxender, C.F. Fox (Eds.), Protein Engineering, Alan R. Liss, New York, 1987, p. 213.
[10] J.C. Leer, K. Hammer-Jespersen, M. Schwartz, Eur. J. Biochem. 75 (1977) 217.
[11] A. Vita, A. Amici, T. Cacciamani, M. Lanciotti, G. Magni, J. Biochem. 18 (1986) 431.
[12] W.J. Cook, G.W. Kosalka, W.W. Hall, S.V.L. Narayana, S.E. Ealick, J. Biol. Chem. 262 (1987) 2852.
[13] L. Walton, C.A. Richards, L.P. Elwell, Nucl. Acids Res. 17 (1989) 6741.
[14] V.L. Tsuprun, I.L. Tagunova, E.V. Linkova, A.S. Mironov, Biokhimiya 56 (1991) 930.
[15] E.Y. Morgunova, A.M. Mikhailov, A.A. Komissarov, C. Mao, E.V. Linkova, A.S. Mironov, A.N. Popov, S. Armstrong, A.A. Burlakova, D.V. Romanova, E.V. Blagova, E.A. Smirnova, V.G. Debabov, S.E. Ealick, Kristallografiya 40 (1995) 672.
[16] E.Y. Morgunova, A.M. Mikhailov, A.N. Popov, E.V. Blagova, E.A. Smirnova, B.K. Vainshtein, C. Mao, S.R. Armstrong, S.E. Ealick, A.A. Komissarov, E.V. Linkova, A.A. Burlakova, A.S. Mironov, V.G. Debabov, FEBS Lett. 367 (1995) 183.
[17] J.M. Sánchez-Ruiz, J.L. Lopéz-Lacomba, M. Cortijo, P.L. Mateo, Biochemistry 27 (1988) 1648.
[18] F. Conejero-Lara, J.M. Sánchez-Ruiz, P.L. Mateo, F.J. Burgos, J. Vendrell, F.X. Avilés, Eur. J. Biochem. 200 (1991) 663.
[19] J.M. Sanchez-Ruiz, Biophys. J. 61 (1992) 921.
[20] B.I. Kurganov, A.E. Lyubarev, J.M. Sánchez-Ruiz, V.L. Shnyrov, Biophys. Chem. 69 (1997) 125.
[21] J.M. Sanchez-Ruiz, J.L. Lopez-Lacomba, P.L. Mateo, M. Vilanova, M.A. Serra, F.X. Aviles, Eur. J. Biochem. 176 (1988) 225.
[22] M. Guzmán-Casado, A. Parody-Morreale, P.L. Mateo, J.M. Sánchez-Ruiz, Eur. J. Biochem. 188 (1990) 181.
[23] P.E. Morin, D. Diggs, E. Freire, Biochemistry 29 (1990) 781.
[24] J.R. Lepock, A.M. Rodahl, C. Zhang, M.L. Heynen, B. Waters, K.-H. Cheng, Biochemistry 29 (1990) 681.

[25] D.I. Kreimer, V.L. Shnyrov, E. Villar, I. Silman, L. Weiner, Protein Sci. 4 (1995) 2349.
[26] A.L. Garda-Salas, R.I. Santamara, M.J. Marcos, G.G. Zhadan, E. Villar, V.L. Shnyrov, Biochem. Mol. Biol. Int. 38 (1996) 161.
[27] V.L. Shnyrov, M.J. Marcos, E. Villar, Biochem. Mol. Biol. Int. 39 (1996) 647.
[28] J.R. Lepock, K.P. Ritchie, M.C. Kolios, A.M. Rodahl, K.A. Heinz, J. Kruuv, Biochemistry 31 (1992) 12706.
[29] D. Milardi, C. La Rosa, D. Grasso, Biophys. Chem. 52 (1994) 183.
[30] S.R. Tello-Solis, A. Hernandez-Arana, Biochem. J. 311 (1995) 969.
[31] C. La Rosa, D. Milardi, D. Grasso, R. Guzzi, L. Sportelli, J. Phys. Chem. 99 (1995) 14864.
[32] R. Guzzi, C. La Rosa, D. Grasso, D. Milardi, L. Sportelli, Biophys. Chem. 60 (1996) 29.
[33] A.M. Mikhailov, E.A. Smirnova, V.L. Tsuprun, I.V. Tagunova, B.K. Vainstein, E.V. Linkova, A.A. Komissarov, Z.Z. Siprashvili, A.S. Mironov, Biochem. Int. 26 (1992) 607.
[34] U.K. Laemmli, Nature 277 (1970) 680.
[35] J.C. Leer, K. Hammer-Jespersen, M. Schwartz, Eur. J. Biochem. 75 (1977) 217.
[36] M.M. Bradford, Anal. Biochem. 2 (1976) 248.
[37] J.A. Nelder, R. Meed, Comput. J. 7 (1965) 308.
[38] K. Takahashi, J.M. Sturtevant, Biochemistry 20 (1981) 6185.
[39] S.A. Aivazyan, I.S. Yenyukov, L.D. Meshalkin, Applied Statistics, Study of Relationships, Finansy i statistika, Moscow, 1985.
[40] D. Grasso, C. La Rosa, D. Milardi, S. Fasone, Thermochim. Acta 265 (1995) 163.
[41] A. Hernández-Arana, A. Rojo-Domínguez, M.M. Altamirano, M.L. Calcagno , Biochemistry 32 (1993) 3644.